

The Ribonucleic Complex HuR-MALAT1 Represses CD133 Expression and Suppresses Epithelial-Mesenchymal Transition in Breast Cancer

Elisa Latorre^{1,2}, Stephana Carelli², Ivan Raimondi³, Vito D'Agostino¹, Ilaria Castiglioni¹, Chiara Zucal¹, Giacomina Moro⁴, Andrea Luciani⁴, Giorgio Ghilardi^{2,4}, Eleonora Monti^{2,4}, Alberto Inga³, Anna Maria Di Giulio², Alfredo Gorio², and Alessandro Provenzani¹

Abstract

Epithelial-to-mesenchymal transition (EMT) is a core process underlying cell movement during embryonic development and morphogenesis. Cancer cells hijack this developmental program to execute a multi-step cascade, leading to tumorigenesis and metastasis. CD133 (PROM1), a marker of cancer stem cells, has been shown to facilitate EMT in various cancers, but the regulatory networks controlling CD133 gene expression and function in cancer remain incompletely delineated. In this study, we show that a ribonucleoprotein complex including the long noncoding RNA MALAT1 and the RNA-binding protein HuR (ELAVL1) binds the CD133 promoter region to regulate its expression. In luminal nonmetastatic MCF-7 breast cancer cells, HuR silencing was sufficient to upregulate N-cadherin (CDH2) and CD133 along

with a migratory and mesenchymal-like phenotype. Furthermore, we found that in the basal-like metastatic cell line MDA-MB-231 and primary triple-negative breast cancer tumor cells, the repressor complex was absent from the CD133-regulatory region, but was present in the MCF-7 and primary ER+ tumor cells. The absence of the complex from basal-like cells was attributed to diminished expression of MALAT1, which, when overexpressed, dampened CD133 levels. In conclusion, our findings suggest that the failure of a repressive complex to form or stabilize in breast cancer promotes CD133 upregulation and an EMT-like program, providing new mechanistic insights underlying the control of prometastatic processes. *Cancer Res*; 76(9): 2626–36. ©2016 AACR.

Introduction

The misactivation of the embryonic dedifferentiation program, epithelial-to-mesenchymal transition (EMT) increases cancer cell motility and dissemination (1), and transient EMT is considered the first essential step in metastasis formation (2). During this complex process, EMT promotes dedifferentiation, growth arrest, migration and invasion of cancer cells, and directly inhibits proliferation by the activation of specific transcription factors of the TWIST, SNAIL, and ZEB families (1–3). One of the recently identified pathways triggering the EMT program stems from the transmembrane protein CD133, and signals through SRC and ERK1/2 (4–6).

CD133 (PROMININ1) is widely recognized as one of the general cancer stem cell (CSC) marker in several cancer types, including breast (7), together with the CD44^{high}/CD24^{low} signature (8). CD133 has a prognostic role in breast cancer (9, 10) and, additionally, its expression has been associated with vascular mimicry capability of triple-negative breast cancer (TNBC) cell lines (11), correlating its presence to more metastasis-prone basal-like cancers. CD133 gene regulation and function in the EMT is still poorly investigated in breast cancer. In this study, we show that a newly identified molecular complex, scaffolded by the long noncoding (lnc) RNA MALAT1 (metastasis associated lung adenocarcinoma noncoding-transcript 1) and comprising the RNA binding protein HuR, regulates CD133 gene expression in dedifferentiating breast cancer cells, both *in vitro* and *in vivo*.

¹Laboratory of Genomic Screening, Center for Integrative Biology, University of Trento, Trento, Italy. ²Laboratory of Pharmacology, Department of Health Sciences, University of Milan, Milan, Italy. ³Laboratory of Transcriptional Networks, Center for Integrative Biology, University of Trento, Trento, Italy. ⁴San Paolo Hospital, Milan, Italy.

Note: Supplementary data for this article are available at Cancer Research Online (<http://cancerres.aacrjournals.org/>).

S. Carelli and I. Raimondi contributed equally to this article.

Corresponding Authors: Elisa Latorre, University of Milan, via Di Rudini, 8, Milan 20142, Italy. Phone: 3902-5032-3039; Fax: 3902-5032-3033; E-mail: elisa.latorre@unimi.it; and Alessandro Provenzani, Center for Integrative Biology, via Sommarive 9, University of Trento, Trento 38123, Italy. Phone: 3904-6128-3094; Fax: 3904-6128-3997; E-mail: alessandro.provenzani@unitn.it

doi: 10.1158/0008-5472.CAN-15-2018

©2016 American Association for Cancer Research.

MALAT1 is one of the most widely studied lncRNA with a strong relation to cancer development and progression. MALAT1 is overexpressed in several solid tumors, and its expression correlates with metastasis in lung cancer (12), but the roles of this lncRNA in the EMT process are not completely defined. MALAT1 is highly abundant in the nucleus (13), and its presence in nuclear speckles has been associated with the activity of RNA polymerase II, recruitment chromatin SR splicing factors (14), and Polycomb-2 protein (15). A genome-wide screening experiment revealed the binding to the lncRNA MALAT1 of the RNA-binding protein HuR (16), but the implications of this binding remain unknown so far.

The human antigen R (HuR; or ELAV1) is a member of the embryonic lethal abnormal vision RNA-binding protein family, known to regulate the half-life of target mRNAs (17). Initially

identified as an mRNA export factor (18), its main nuclear functions are regulation of splicing, mRNA processing, and polyadenylation (19). In this work, we identified the chromatin-associated HuR/MALAT1 functional complex, during the dedifferentiation process of cancer cells, which controls CD133 gene expression, both *in vitro* and *in vivo*. HuR/MALAT1 impact on CD133 gene expression can regulate EMT phenotype features, suggesting that the fine regulation of these molecules could control, at least in part, tumor progression.

Materials and Methods

Cell lines

The MCF-7 and MDA-MB-231 breast cancer cell lines, purchased and authenticated (STR profiling) from Interlab Cell Line Collection were kept in culture for no more than 2 months in DMEM, 10% FCS. Mammosphere cells were cultured in F12/DMEM (1:1) supplemented with B27 (Invitrogen), 20 ng/mL recombinant human EGF (R&D Systems), 20 ng/mL recombinant human basic-FGF (R&D Systems), 100 U/mL penicillin, 100 µg/mL streptomycin, and 5 µg/mL heparin. Floating aggregates were considered mammospheres when diameter >60 µm.

Primary cell culture

Human breast carcinoma specimens were obtained from the Oncology Unit, San Paolo Hospital (Milan, Italy). Tumor samples were processed within 1 hour after surgical resection, washed with F12/DMEM (1:1) medium, minced with a sterile scalpel, and placed in digestion medium (DMEM/F-12) supplemented with 200 U/mL collagenase A (Stem Cell Technologies) and 100 U/mL hyaluronidase (Stem Cell Technologies) for 1 hour at 37°C.

Cell growth and invasion

The total number of cells in each culture passage was measured, after mechanical dissociation, by Tali image based cytometer (Life Technologies). Results were displayed as log10 of the total number of cells. Cell invasion ability was assessed by QCM fluorimetric cell migration assay kit (ECM509, Chemicon) as per manufacturer's recommendations.

PKH26 staining

Scrambled and knockdown (KD) HuR MCF-7 cells were cultured under mammosphere culture conditions, washed in PBS, and stained with PKH26 (M0973, Sigma). Epifluorescence was measured by BD FACScanto flow cytometer after 8 culture passages (20).

Immunocytochemistry

After cultivation on acid-washed glass coverslips, cells were treated and fixed. The following antibodies were used: anti-HuNu (Millipore, MAB1281), anti-HuR (SC71290, Santa Cruz Biotechnology), and anti-HDAC6 (AB88494, Abcam)

RNA FISH

FISH was adapted from ref. 21. Sense and antisense AlexaFluor 488-labeled RNA probes (Ullysis Nucleic Acid Labeling Kit; Life Technologies) were synthesized from a MALAT1-amplified sequence. The cDNA sequence was verified by sequencing.

Soft agar assay

Mammospheres obtained from parental and KD HuR MCF-7 were suspended 2,500 cells/cm² in 0.3% agarose with mammosphere culture medium on a 0.8% agar base layer and covered with culture medium. Colonies >50 µm diameter were counted and quantified by ImageJ software.

Quantitative real-time PCR

Total RNA from cultured cells and tissue samples were isolated using TRIzol Reagent (Invitrogen). Total RNA (1 µg) was reverse transcribed using iScript cDNA Synthesis Kit (Bio-Rad) according to the manufacturer's instructions. qRT-PCR was performed with an DNA engine OPTICON2 detection system (MJ Research) using iQ SYBR Green Supermix (Bio-Rad).

Western blot analysis

Whole cell lysates were used for Western blotting performed in denaturing conditions on polyvinylidene difluoride (PVDF) membrane following Laemmli SDS-page procedure. Anti-HuR (SC365816, Santa Cruz Biotechnology), anti-HDAC6 (AB1440, Abcam), anti-CD133 (130105226, Miltenyi Biotec), anti-N-cadherin (610920, BD Biosciences), anti-E-cadherin (3195, Cell Signaling Technology), and anti-histone H3 (AB1791, Abcam), anti-LDH (ABN311, Millipore), ST1011 (Millipore), and anti-β-actin (A5441, Sigma) antibodies were used. Signal detection was performed by HRP-conjugated secondary antibody and ECL solutions (RPN2108, GE Healthcare). Images were taken with Geldoc XR (Bio-Rad).

Cell migration assay by xCELLigence

Cell migration was monitored in real-time using xCELLigence system. Cells were seeded in a CIM-Plate 16 in triplicate and the migration behavior of each was monitored for 48 hours. Cells maintained in serum-free media served as a control.

IHC

Five-micron thick sections representative of the tumor were immunostained using the Super Sensitive Non-Biotin HRP Detection System (34002, Thermo Scientific), with the anti-human Nuclei (HuNu; MAB1281, Millipore). Eosin (230251, Sigma) staining was used as counterstaining. Controls consisting of alternate sections incubated by omitting the primary antibody did not show any detectable immunoreactivity.

RNA immunoprecipitation

RNA was isolated from the different samples by TRIzol as per the manufacturer's recommendations, retrotranscribed into cDNA by MBI-Fermentas kit, and used as a template for PCR analysis (22).

Capture hybridization analysis of RNA targets

Cross-linked and sonicated nuclear cell extract was incubated with C-oligo, sense-oligo, or without probes and hybridized overnight. Hybridized material was captured with magnetic streptavidin resin (Invitrogen). Bound material was washed, eluted with RNase H, and crosslinking was reversed at 65°C over night, and DNA and protein were purified by phenol:chloroform:isoamyl alcohol precipitation or boiled 5' in Laemmli buffer, respectively. MALAT-1 binding and specificity of used C-oligos and all following steps were performed as described previously (23).

Latorre et al.

ChIP and RT-on-ChIP

Chromatin immunoprecipitation (ChIP) was performed following previously published protocols (24). In reverse transcription PCR on ChIP (RT-on-ChIP) experiments, the immunoprecipitation protocol was performed in the presence of RNase inhibitor and at the end of the elution step, the samples were reverse transcribed using iScript cDNA Synthesis Kit (Bio-Rad) according to the manufacturer's instructions and analyzed by PCR.

Xenotransplantation

Scrambled and *Hur* knocked down (HuR-KD) cells were cultured under mammosphere culture conditions, washed with PBS and stained with PKH26 (M0973 Sigma), and resuspended in PBS/Matrigel mixture (1:1 volume). A measure of 5×10^6 cells in 0.1 mL of this mixture was implanted in the mammary fat pad of 5-week-old female athymic nude Fox1nu mice (Harlan Laboratories). The mice received β -estradiol (E2758, Sigma) supplementation (0.4 mg/kg) every 7 days. Animal experimentation was performed according to the protocol 2/2013 approved by the local ethical committee.

Anoikis test

Anoikis assay (25) was performed by seeding MCF-7 cells at 1×10^5 cells/mL in either DMEM complete medium or in mammosphere forming medium. Cyclosporin-A (30024, Sigma) 10 μ mol/L for 24 hours was used as a positive control. Cells were incubated for 24 hours prior to the MTT assay (M5655, Sigma). We tested cell population in adhesion and after 5 days in suspension cultures. MTT signal was normalized to the number of cells and measured by Bradford assay at day 1 and day 5.

Ethical disclosure

The ethical committee of the Department of Health Sciences approved the design of this study, which was carried out according to the guidelines of the University of Milan (Milan, Italy). Specimens from 6 subjects (females between the ages of 66 to 73 years) were kept at the San Paolo Hospital (Milan, Italy). An informed consent was obtained from all the patients. This study was performed in strict accordance with the recommendations in the Guide for the Care and Use of Laboratory Animals of the National Research Council, Italy. The protocol was approved by the Committee on the Ethics of Animal Experiments of the University of Milan (Milan, Italy).

Additional and detailed materials and methods are provided in the "online Supplementary Material" section.

Results

HuR-stable silencing leads to adhesion increase and cell proliferation decrease of mammospheres

To characterize the role of HuR in maintaining the mesenchymal state of cancer cells, we generated mammospheres from MCF-7, in which HuR was stably ablated (HuR-KD; ref. 26; Supplementary Fig. S1A and S1B). Cumulative cell counts of HuR-KD mammospheres at passage 8 revealed a reduced number of cells, compared with the control (scrm). The higher degree of PKH26 staining retention in HuR-KD mammospheres pointed to a slower rate of cell proliferation, and not to a differential resistance to anoikis (Fig. 1A and Supplementary

Fig. S2). Moreover, HuR-KD mammospheres were higher in number but smaller in dimension than control-derived mammospheres (Fig. 1B). We evaluated the ability of HuR-KD mammospheres to adhere to the substrate and migrate or invade. Surprisingly, in cell motility tests, HuR-KD mammospheres reached significantly higher values compared with the parental population, in the absence of serum, (Fig. 1C and Supplementary Fig. S3A). In anchorage-independent condition, HuR-KD mammospheres grew slowly, as smaller colonies than wild-type cells were formed in soft agar at fixed time points (Fig. 2A). However, when HuR-KD cells were allowed to grow until the colonies reached a fixed dimension, we counted the same number of colonies as for the wild-type cells, again suggesting a decrease in proliferation rate, and not in clonogenic survival. To evaluate the tumorigenic potential of disaggregated cells from HuR-KD mammospheres, we injected dilutions of cells (5×10^2 – 5×10^6) orthotopically in the mammary fat pad of the recipient female nude mice and monitored the onset and dimension of the derived tumors (Fig. 2B and Supplementary Fig. S3B–S3D). Cells from both types of mammospheres generated tumors in the 45 days dedicated to the observation, but those from HuR-KD mammospheres gave rise to significantly smaller tumors in comparison with the control, confirming the reduced proliferation rate of HuR-KD cells, but equivalent tumorigenic potential. HuR-KD cells displayed high N-cadherin and CD133 expression levels compared with the wild-type, suggesting that genetic ablation of HuR can affect the EMT outcome. As CD133 regulates N-cadherin expression (6), we silenced CD133 (CD133 KD; Fig. 2C and Supplementary Fig. S4A) in wild-type and HuR-KD MCF-7 cells. Interestingly, CD133 silencing in HuR-KD cells reduced N-cadherin expression to the wild-type level, suggesting a role for HuR in CD133-dependent EMT. In summary, HuR-KD mammospheres show the same tumorigenic potential as wild-type population, but HuR silencing enforces a mesenchymal phenotype by increasing cell migration together with the decrease in cell proliferation.

HuR depletion increases CD133 expression without binding its mRNA

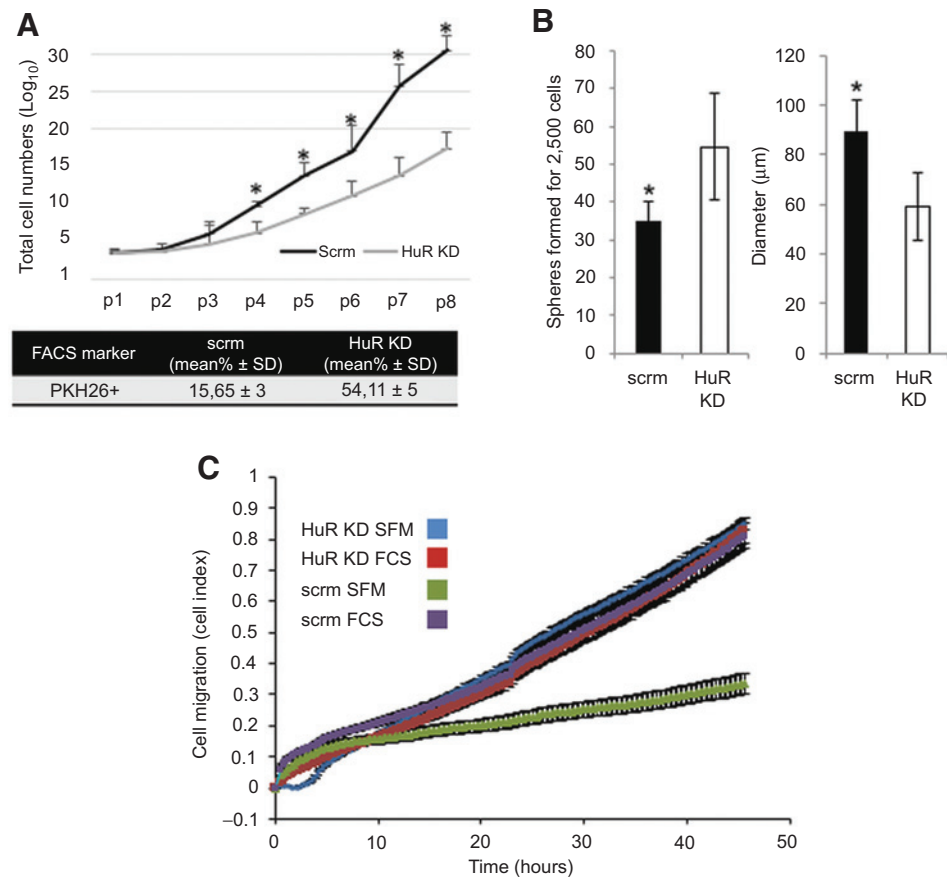
As the overexpression of N-cadherin was CD133 dependent in HuR-KD mammospheres, we investigated whether HuR was directly regulating CD133 mRNA. A significant increment of CD133 mRNA and protein expression was observed in the entire HuR-KD population, compared with control (Fig. 2D). HuR is known for its ability to bind the 3'UTR of mRNA molecules regulating their half-life and translation (27), but, by RNA immunoprecipitation assay (RIP), we did not find any significant fold increase of CD133 mRNA in the HuR-bound material (Supplementary Fig. S4B).

HuR binding to CD133 promoter region in MCF-7 mammospheres requires MALAT1

We then wondered whether HuR was binding to the *CD133* gene, using ChIP both in adherent cells and in mammospheres. We probed four different positions (A, B, C, and D region) and found HuR bound to the one (D), within the second intron of the *CD133* gene, but only in mammospheres originating from MCF-7. We did not observe this binding in mammospheres derived from MDA-MB-231 breast cancer cells, where *CD133* gene is transcribed at a higher level than MCF-7 cells (Fig. 3A). The

Figure 1.

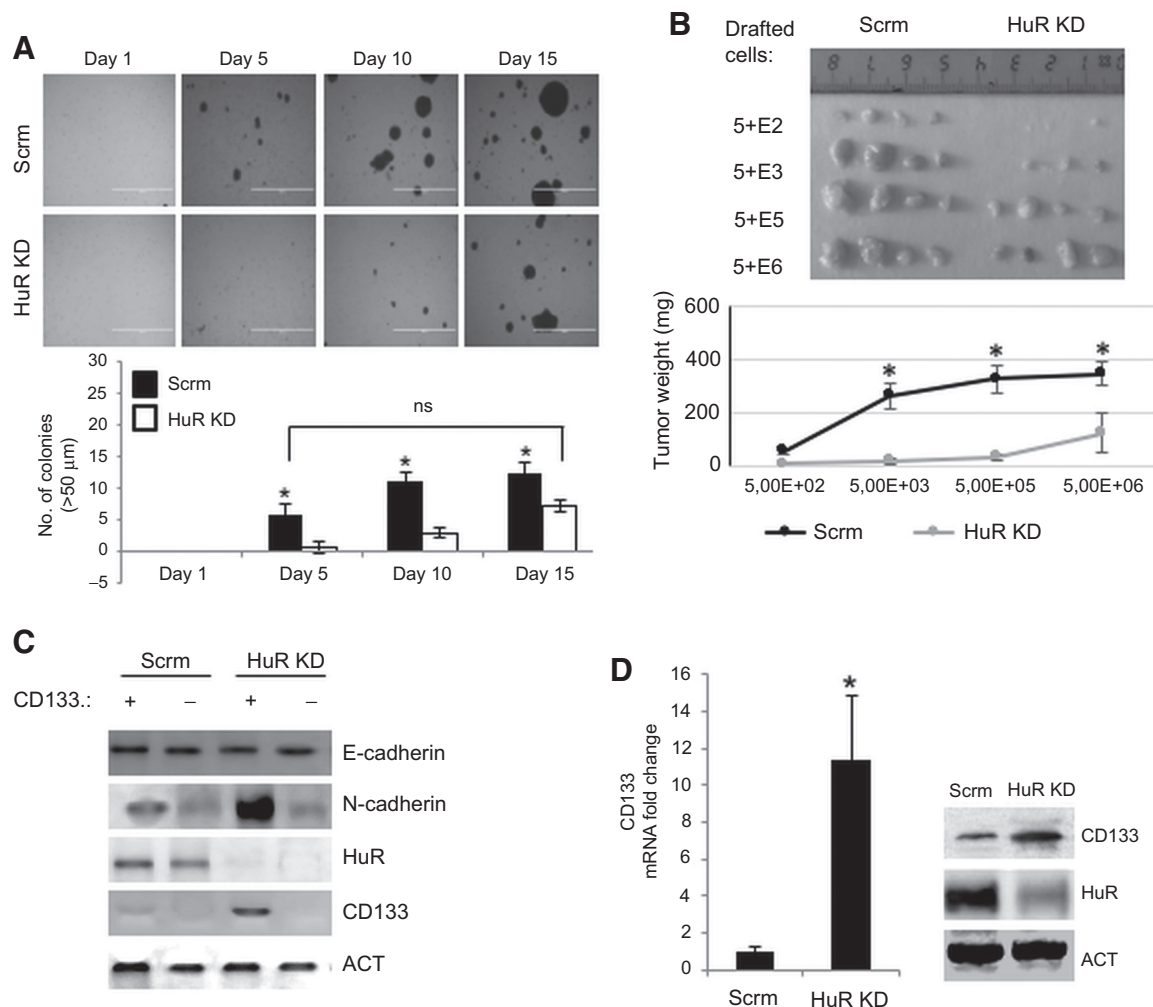
HuR-KD mammospheres cellular are less proliferating but more migrating than wild-type mammospheres. A, cell growth curves of scrambled wild-type mammospheres (scrm) and HuR silenced (HuR-KD) mammospheres reported as total cell number counted at each culture passage (p1-p8, every four days; top). Bottom, PKH26 staining of MCF-7 mammospheres as a percentage of positive cells. *, $P < 0.01$ in t test. B, mammosphere number and diameter of HuR-KD (white bar) and control scrm (black bar) MCF-7 cells after 15 culture days by 2,500 seeded cells. *, $P < 0.01$ in t test. C, xCELLigence migration/adhesion plot of HuR-silenced (HuR-KD) and scrambled control (scrm) mammospheres. Cells were cultured and monitored for surface adhesion (cell index) for 45 hours in the presence (FCS) or absence (SFM) of serum. The HuR-KD cells in the presence (red dot) or absence (blue dot) of serum adhere to the surface, instead scrm adhere only in the presence of serum (purple dot) and fail adhesion in serum-free condition (green dot).



primers used to probe region D amplify a 234 bp long fragment from base 16077104 to base 16077337 of chromosome 4 (GRCh37), within the second intron of the *CD133* gene. Notably, in adherent cells, HuR was bound to a promoter region of the *CD133* gene (A). We evaluated whether the binding detected by ChIP was RNA-dependent (28): RNAse digestion abrogated HuR binding to both regions A (in adherent cells) and D (in mammospheres) of the *CD133* gene. HuR binds to several lncRNAs, such as linc-p21, linc-MD1, and MALAT1 (16, 29, 30). MALAT1 has been shown to scaffold ribonucleoprotein complexes on the chromatin to regulate gene expression (31, 32) and is overexpressed in mammospheres compared with adherent cells while linc-p21 expression was not affected by the adhesion condition (Fig. 3B). According to this, we hypothesized that the RNA molecule responsible for HuR binding is MALAT1. Strikingly, genetic ablation by siRNA against MALAT1 abolished HuR binding to the *CD133* D region in mammospheres, but not to the *CD133* A region in adherent cells (Fig. 3A). MALAT1 is mainly a nuclear lncRNA molecule (Fig. 3C; refs. 33, 34) and is bound by HuR (Fig. 3D). To validate the presence of the complex on the *CD133* D region, we performed capture hybridization analysis of RNA targets (CHART; ref. 35). MALAT1 was bound to the regulatory region of its gene (32), our positive control, and, on the *CD133* gene A region, but weakly on the *CD133* gene D region, and not on the *ACTIN* gene, used as negative control (Fig. 4A, top). In mammospheres, MALAT1 appeared to be bound to the D region and not to the A region (Fig. 4A, bottom). Moreover,

analyzing MALAT1 pull-down protein fraction during CHART, we observed the presence of HuR, validating its binding to MALAT1 on the chromatin, only in mammospheres (Supplementary Fig. S5). This result is in agreement with ChIP data and supports the copresence of HuR and MALAT1 on the D chromatin region in mammospheres, and in A region in adherent cells. MALAT1 was present alone on the D region, but with much less confidence and to a lower extent than to the A region, in adherent condition (Fig. 4A). Therefore, the additional contribution of HuR is important for stabilizing MALAT1 binding to this region, and, at the same time, its ability in binding the chromatin also in the absence of HuR, possibly together with other trans-factors. HuR binding to the A region in adherent cells is MALAT1 independent, but RNA-dependent, indicating additional mechanisms of position-specific recruitment of HuR on the *CD133* locus. In mammospheres, we also checked for the presence of MALAT1 RNA in the HuR ChIP samples by RT-PCR (RT-on-ChIP) showing the existence of the HuR-MALAT1 assembly in the nucleus (Fig. 4B). Either HuR or MALAT1 silencing induced the upregulation of the *CD133* protein expression level (Figs. 2D and 4C), and of the downstream molecule N-cadherin (Fig. 4D) showing the functional relevance of the HuR/MALAT1 complex. Moreover, MALAT1 downregulation did not affect HuR expression level (Fig. 4D). Therefore, HuR and MALAT1 recruited within the second intron of *CD133* gene to the chromatin exclusively in MCF-7 mammospheres, limiting the expression of the gene.

Latorre et al.

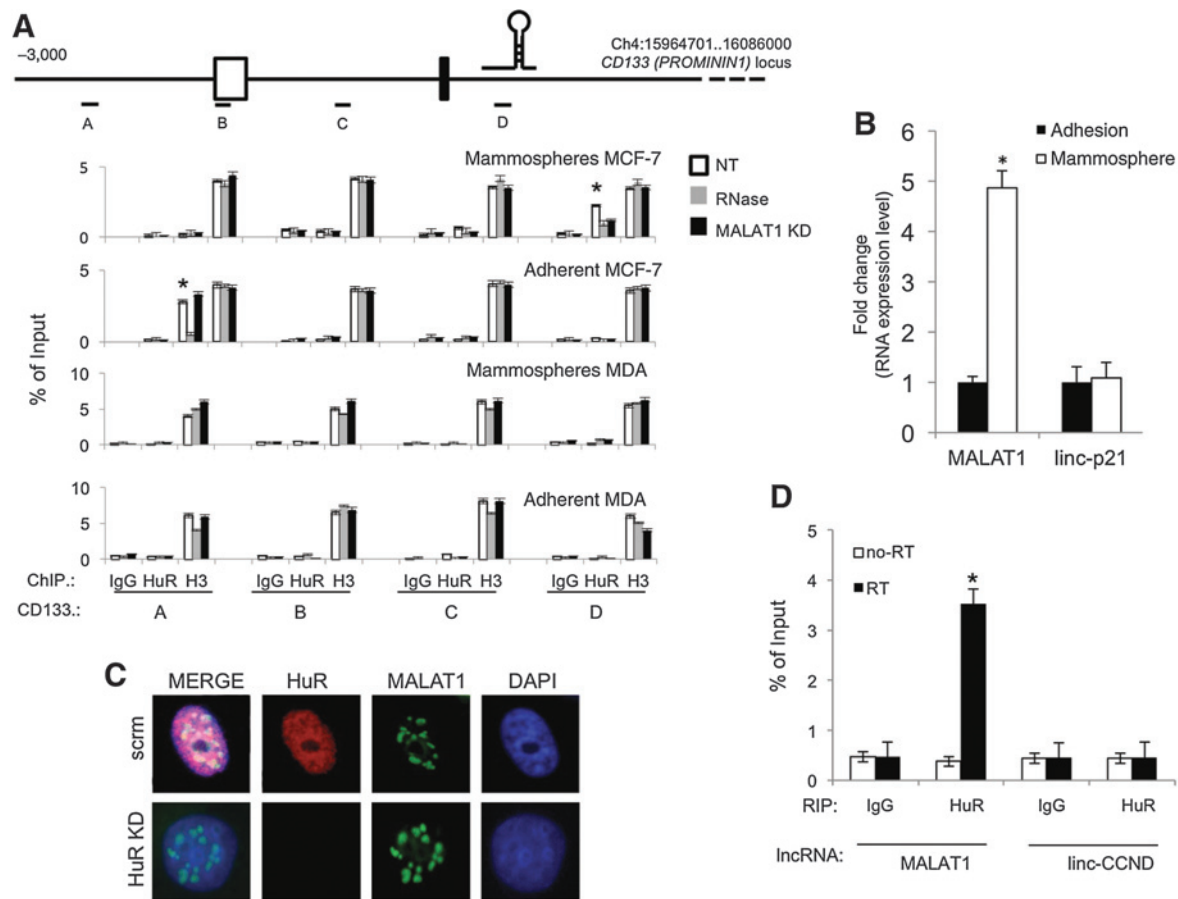
**Figure 2.**

HuR ablation in mammospheres decreases tumor dimension but increases CD133-dependent N-cadherin expression. A, soft agar colony formation of scrambled (scrm) and HuR-silenced (HuR-KD) mammospheres. Top, direct light pictures of the cultures at different time points (day 1–15). Bottom, histogram gives a quantification of the colony formed by scrm (black bar) and HuR-KD (white bar). Scrm colonies at day 5 reached a similar size as HuR-KD cells at day 15. *, $P < 0.01$, t test. B, the picture shows the tumors surgically removed from female nude mice orthotopically xenotransplanted in the mammary fat pad with scrambled (scrm) and HuR-silenced (HuR-KD) mammospheres. Surgery was performed with different dilution of cells (from 5×10^2 – 5×10^6). The graph shows the tumor weight (mg) originated from the two cell types. *, $P < 0.01$. C, Western blots showing the expression of E-cadherin, N-cadherin, HuR, and CD133 in parental (scrm) or HuR-KD MCF-7 mammospheres in which CD133 expression was transiently ablated (CD133 KD). β -Actin was used as a loading control. HuR-KD displayed higher CD133 and N-cadherin compared with the parental. CD133 silencing reverted N-cadherin expression to the parental level in HuR-KD. D, the histogram shows CD133 mRNA expression levels in scrambled (scrm) and HuR-silenced (HuR-KD) mammospheres. mRNA levels were determined by qRT-PCR and are reported as $2^{-\Delta(\Delta C_t)}$, where the housekeeping genes were 18S and GAPDH. Values were plotted as mean \pm SD from three independent experimental replicates. *, $P < 0.01$ in t test. Right, Western blotting showing CD133 protein expression level in HuR-KD mammospheres in comparison with control (scrm). Actin was used as loading control.

Differential association of the HuR/MALAT1 complex on the CD133 gene in ER⁺ and TNBCs

We compared MCF-7 cells, a model for luminal (epithelial) breast cancer, with MDA-MB-231 cells, defined as basal-like invading (mesenchymal) breast cancer (35). The protein level of EMT markers, in mammospheres derived from MDA-MB-231 cells, showed high N-cadherin and low E-cadherin expression, compared with MCF-7 mammospheres (scrm). The same was observed with mammospheres derived from primary ER⁺ (luminal) or TNBC (basal-like) tumor cells (Fig. 5A; Supplementary Table S1). CD133 was higher in MDA-MB-231 and TNBC primary

cells, as in the HuR-KD MCF-7 cells, compared with the parental MCF-7 and the ER⁺ primary cells (Fig. 5A). HuR expression was comparable between MCF-7 and MDA-MB-231 or ER⁺ and TNBC primary cells (Fig. 5A). CD133 was overexpressed in mammospheres derived from MDA-MB-231 cells, and in TNBC when compared with the MCF-7 cells and ER⁺ samples. Notably, MALAT1 had an opposite trend of expression to CD133 while HuR levels did not change (Fig. 5B and C). We ectopically overexpressed MALAT1 in MDA-MB-231, observing CD133 and N-cadherin downregulation (Fig. 5E and F) according to the HuR-MALAT1 complex repression activity.

**Figure 3.**

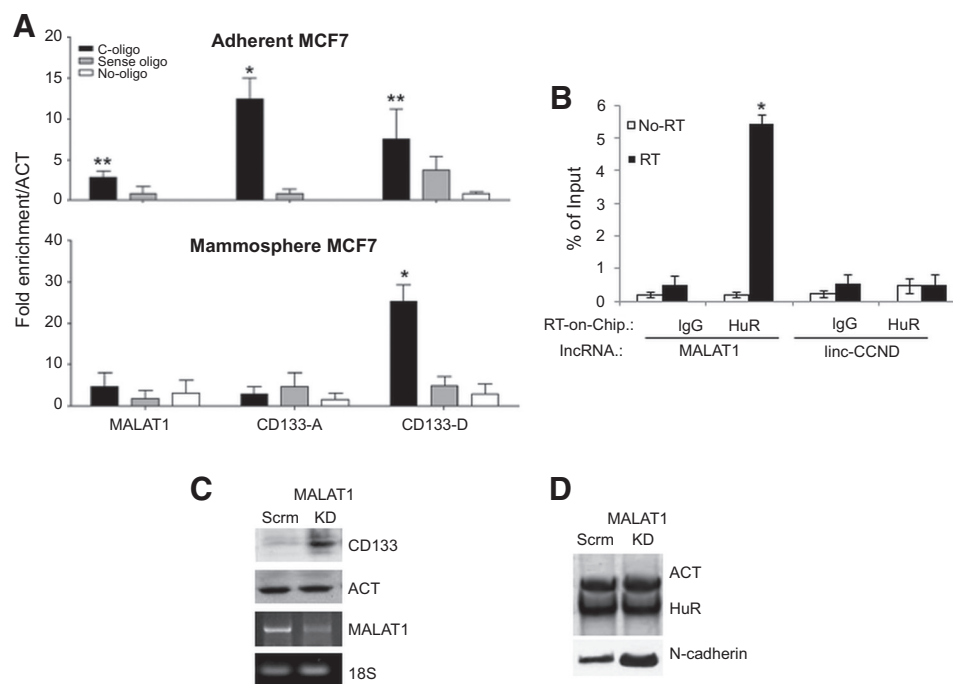
HuR interacts with MALAT1 and binds to the *CD133* gene in mammospheres only. A, top, map showing *prominin1* locus. Black and white (5'UTR) boxes, exons. The small black bars named from A-D refer to the regions. The RNA hairpin is representative of MALAT1. Bottom, ChIP was performed with MCF-7 and MDA-MB-231 as mammospheres or in adhesion. HuR binding to *CD133* gene regions named A, B, C, and D was tested. Results are reported in the histogram as input percentage (% of input) of the fold enrichment measured by densitometry. PCR was performed with (RNase, gray bar) or without RNase treatment (NT, white bar) or after MALAT1 RNA silencing (MALAT, black bar). Preimmunization serum (IgG) was used as precipitation negative control. Anti-histone-H3 was used as positive control. Densitometric values were plotted as mean \pm SD from independent experimental triplicates. *, $P < 0.01$ in *t* test. B, the histogram shows MALAT1 and linc-p21 RNA expression level in MCF-7 cells grown in adhesion (adhesion, black bar) in comparison with mammospheres (mammosphere, white bar). Values were plotted as mean \pm SD from three independent experimental replicates. *, $P < 0.01$ in *t* test. C, immunofluorescence and RNA FISH against HuR (red) and MALAT1 RNA (green) on MCF-7 cells silenced (HuR-KD) or not (scrm) for HuR expression. DAPI was used as counterstaining. D, RIP assay was performed with MCF-7-derived mammospheres to evaluate MALAT1 RNA binding to HuR. The results are reported in the histogram as input percentage (% of input) of the fold enrichment, measured by densitometry. PCR was performed with (black bar) or without retrotranscription (no RT) as amplification negative control (white bar). Preimmunization serum (IgG) was used as precipitation negative control. linc-CCND was used as a negative control. Densitometric values were plotted as mean \pm SD from three independent experimental replicates. *, $P < 0.01$ in *t* test.

To evaluate the generalization of the *CD133*-MALAT1 inverse correlation between ER⁺ and TNBC tumors, we checked public datasets derived from high-throughput sequencing expression profiles (RNA-seq) performed on primary tumors (116 patients, 28 breast cancer cell lines, 42 TNBC primary tumors, 42 ER⁺ and HER2-negative breast cancer primary tumors and 30 uninvolved breast tissue samples). TNBC patients display significantly higher *CD133* expression levels if compared with the ER⁺ ones (GSE58135; Fig. 5D). MALAT1 was upregulated in tumor samples compared with healthy tissues and was downregulated in TNBC compared with ER⁺ tumor samples. However, the difference was not highly significant, suggesting that other parameters can play a role in defining the *CD133* expression. HuR was not found to change in the overall analysis. Normal breast tissue showed a Pearson coefficient (r) = -0.36 , analogous to the ER⁺ breast

cancer tissue samples (r = -0.34) showing a moderate inverse correlation of MALAT1 and *CD133* expression levels. Combining the two datasets, the inverse correlation is even stronger (r = -0.44). TNBC samples lost this inverse correlation (r = 0.016), in good agreement with the absence of MALAT1/HuR on the *CD133* gene, and consequent dysregulation of *CD133* expression level (Table 1).

We performed RIP, RT-on-ChIP, and ChIP analyses on mammospheres derived from three ER⁺ breast cancer patients' primary cells. Indeed, we found the same pattern of chromatin association as in MCF-7 cells: HuR was binding to MALAT1 RNA (Fig. 6A), and the complex was present on the chromatin (Fig. 6B) at the level of the *CD133* D region in an RNA-dependent manner (Fig. 6C). Coherently, the HuR/MALAT1 inhibiting ribonucleic complex was not found to be associated with the *CD133* D region by ChIP

Latorre et al.

**Figure 4.**

Differential binding sites of MALAT1 in mammospheres and MALAT1-dependent CD133 expression. A, MALAT1 ChART enrichment of MALAT1, CD133 locus A, and CD133 locus D DNA assessed by qPCR from adherent MCF-7 cells or MCF-7-derived mammospheres. The readout is expressed as chromatin fold enrichments normalized for the negative control Actin gene. ChART sheared DNA was precipitated in three different conditions with MALAT1-specific RNA probe (C-oligo, black bar), with RNA probe not complementary to MALAT1 (sense-oligo, gray bar) and without probe as a further control (no-oligo, white bar). *, $P < 0.01$; **, $P < 0.05$ in t test. B, RT-on-ChIP was performed on MCF-7-derived mammospheres to detect MALAT1 RNA binding the chromatin bound to HuR. The results are reported in the histogram as input percentage (% of input) of the fold enrichment. PCR was performed with (black bar) or without retrotranscription (no RT) as negative control (white bar). Preimmunization serum (IgG) was used as precipitation negative control. linc-CCND was used as a negative control. Densitometric values were plotted as mean \pm SD from three experimental replicates. *, $P < 0.01$ in t test. C, Western blots showing CD133 protein expression level during MALAT1 silencing (MALAT1) in mammospheres in comparison with scrambled control (scrm). Actin was used as loading control. MALAT1 expression level was measured by semi-qRT-PCR using 18S as loading control. D, Western blots showing HuR and N-cadherin protein expression level during MALAT1 silencing (MALAT1) in mammospheres in comparison with scrambled control (scrm). Actin was used as loading control.

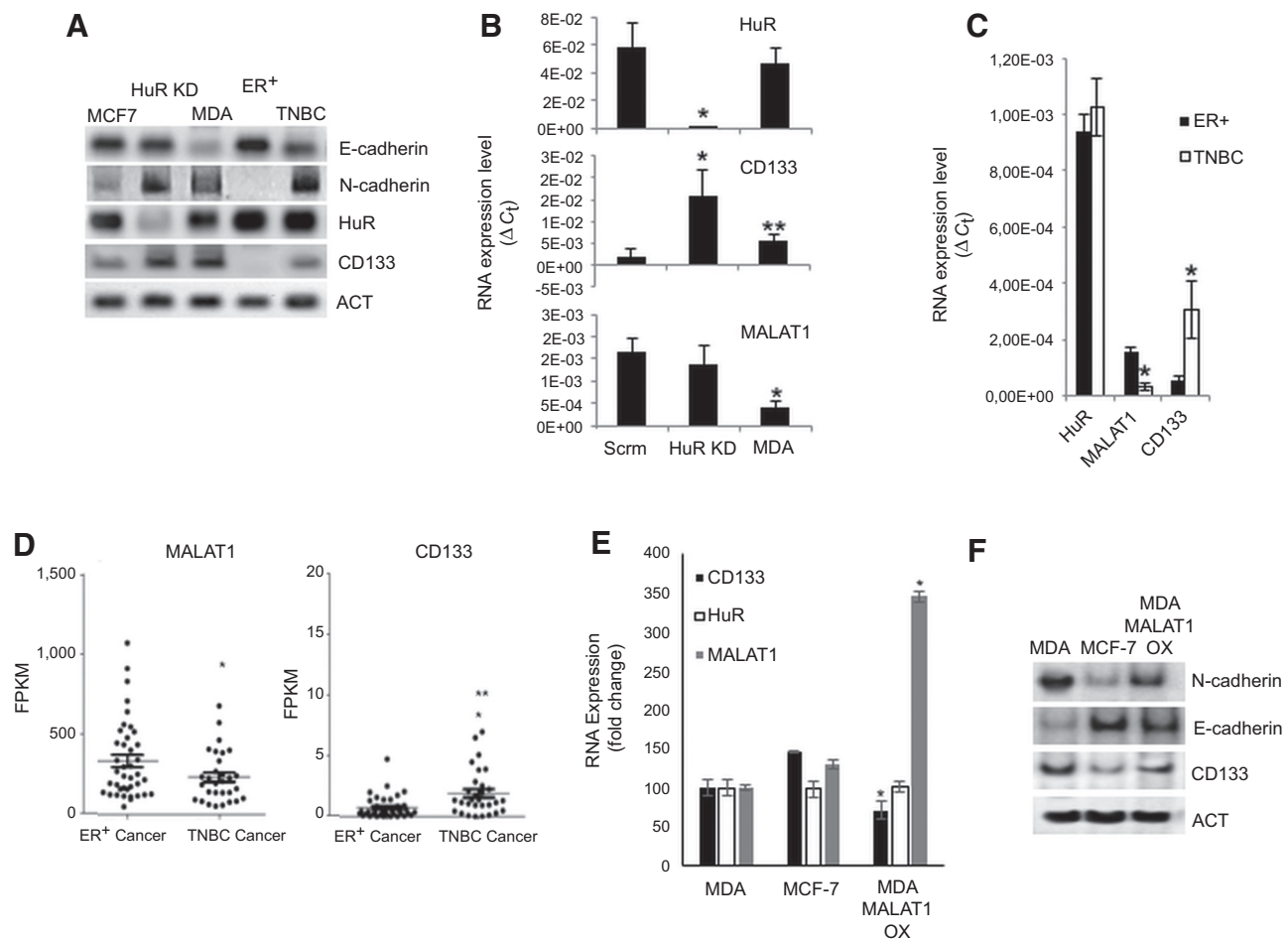
analysis in MDA-MB-231 and TNBC primary cells derived mammospheres (Fig. 6D). Therefore, *CD133* is upregulated in TNBC samples, and the reason for this overexpression partially resides in the downregulation of MALAT1 in TNBC compared with ER⁺ samples. This supports the idea that the fine-tuning of the complex components regulates the expression level of *CD133* gene, affecting EMT phenotype.

Discussion

CD133 plays a crucial role in cancer metastasis acting at the level of EMT in pancreatic ductal adenocarcinoma (4, 6) while its functional role in breast cancer is not well defined. We observed that HuR-stable downregulation in dedifferentiating, nonmetastatic breast cancer cell line (luminal ER⁺ cell model, MCF-7) induced the acquisition of EMT traits, such as a more adhesive and migrating phenotype and, concomitantly, a reduction in proliferation rate. Molecularly, the increase of N-cadherin was explained by the upregulation of *CD133*, which is caused by the detachment of a transcriptional inhibitory complex containing MALAT1/HuR from a *CD133* gene regulatory region in intron 2. MALAT1 is a well characterized predictive marker for metastasis development in lung cancer, where it specifically promotes EMT transition, by regulating the expression level of key prometastatic

genes as *LPHN2*, *ROBO1*, *ABCA1*, and *GPC6* (34, 36). However, much less is known regarding its role in breast cancer EMT, where MALAT1 downregulation is suggested to trigger EMT by regulating *LPHN2*, *ROBO1*, and *GPC6* genes and increasing N-cadherin protein expression in breast cancer cell lines (37). HuR is known to bind lncRNA molecules as linc-MD1 and lincRNA-p21 and posttranscriptionally regulate their function in the cytoplasm (29, 30). We showed that HuR was required in the formation of a chromatin regulatory complex, bearing a lncRNA core with a transcriptional repressive function. Other RBPs, such as the hnRNPK or TLS/FUS proteins (38–40) that form repressive chromatin complexes, in association with linc-RNA-p21 and ncRNA-CCND1, respectively, on gene promoters. In our case, the complex (HuR/MALAT1) is bound to a region within the *CD133* gene second intron, suggesting a variation of the chromatin state, via recruitment of epigenetic modulators, or a different chromatin looping between the adherent and mammosphere cell state.

We showed that genetic downregulation of any components of the complex led to an upregulation of the *CD133* gene, and to the following switch of the ER⁺ breast cancer cells to a more basal-like phenotype. Interestingly, *CD133* is epigenetically regulated and highly expressed in basal-like TNBC (41, 42), and is a concurring cause of the aggressiveness of this breast cancer subgroup (11, 43). Importantly, we did not detect HuR, and its complex, on the

**Figure 5.**

TNBCs show different expression level of MALAT1, CD133, and N-cadherin in comparison with ER⁺ cancers. A, Western blots showing the expression level of E-cadherin, N-cadherin, HuR, and CD133 in mammospheres derived from parental MCF-7 cells (scrm), HuR knocked down MCF-7 cells (HuR-KD), MDA-MD-231 cells, and primary cells from ER⁺ (Patient ID:ER+1) and TNBC (PatientID: TNBC) tumors. β -Actin was chosen as loading control. HuR-KD displayed higher CD133 and N-cadherin like MDA-MB-231 and TNBC. B, qRT-PCR to evaluate HuR, CD133, and MALAT1 expression level in mammospheres derived from MCF-7 cells HuR silenced (HuR-KD) or not (scrm) and MDA-MB-231 cells. *, $P < 0.01$ in t test. C, qRT-PCR to detect MALAT1 RNA expression level in primary cells from ER⁺ (black bar) and TNBC (white bar) tumors (All patients). *, $P < 0.01$ in t test. D, MALAT1 and CD133 expression levels expressed as fragments per kilobase of exon per million fragments mapped (FPKM) obtained for GSE58135 RNA-seq dataset. TNBC patients display an overall lower MALAT1 and a higher CD133 expression levels if compared with the ER⁺ ones. *, $P = 0.0421$; ***, $P = 0.0006$ in Wilcoxon signed-rank test. E, qRT-PCR to evaluate HuR, CD133, and MALAT1 expression level in mammospheres derived from MCF-7 and MDA-MB-231 cells overexpressing MALAT1 (MDA MALAT1 OX) or not (MDA) and MCF-7 cells. Values are expressed as fold change relative to the MDA. *, $P < 0.01$ in t test. F, Western blots showing the expression level of E-cadherin, N-cadherin, and CD133 in mammospheres derived from parental MCF-7 cells and MDA-MD-231 overexpressing or not MALAT1 (MDA MALAT1 OX). β -Actin (ACT) was chosen as loading control. MALAT1 overexpression reduces CD133 and N-cadherin expression in MDA-MB-231.

CD133 gene regulatory region in TNBC cell model (MDA-MB-231) and primary TNBC tumor cells, as we did in ER⁺ cell model (MCF-7) and primary ER⁺ mammosphere tumor cells. Indeed, mammospheres represent a dedifferentiated cell state in which

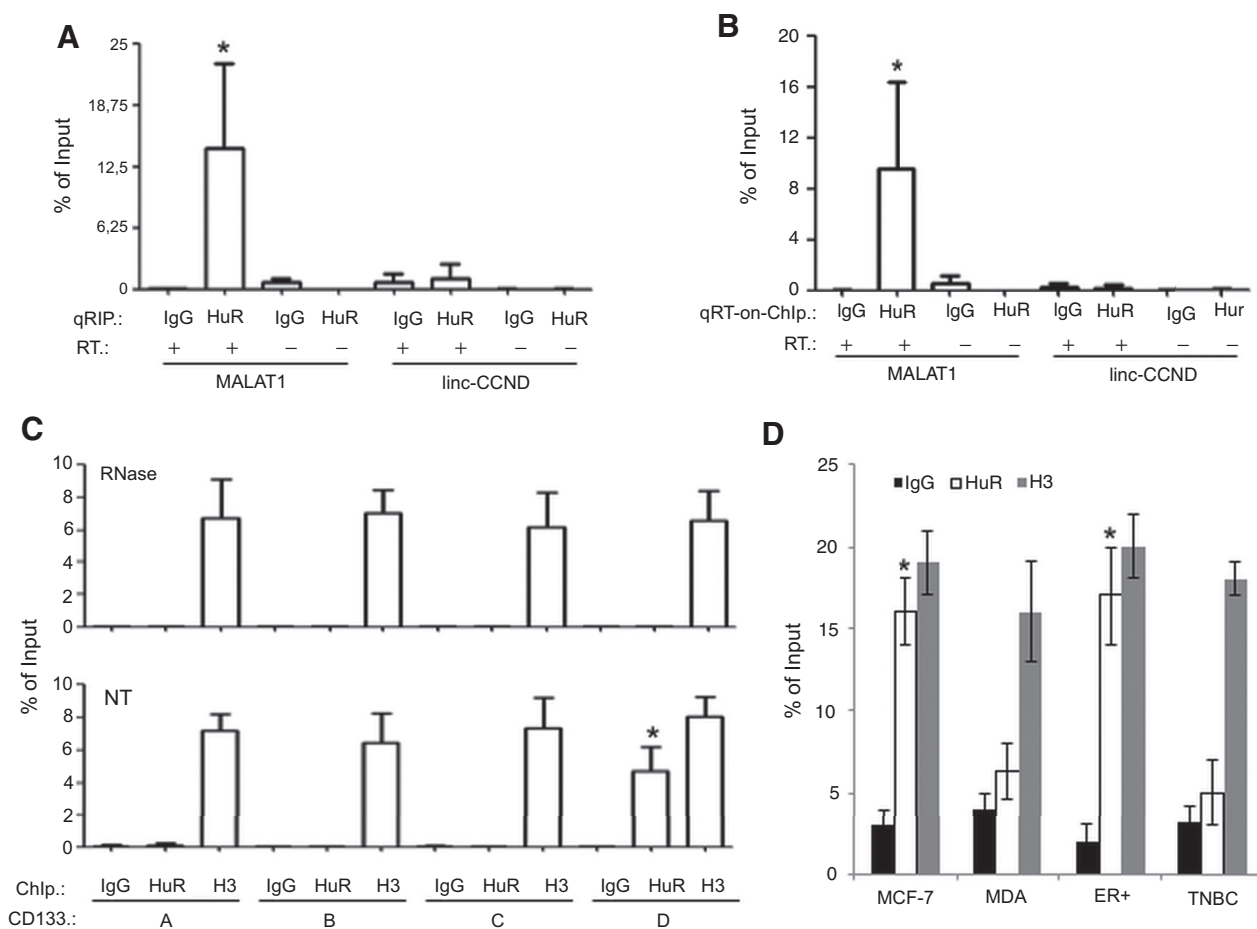
Table 1. The Pearson coefficient for CD133 and MALAT1 expression of the indicated datasets

Dataset samples	Pearson coefficient, r
Normal, adjacent tissue	-0.36
ER ⁺ Her2- tissue	-0.34
Normal adjacent tissue plus ER ⁺ Her2- tissue	-0.44
TNBC	0.016

NOTE: The inverse correlation is moderate for normal, ER⁺, and for the sum of these two datasets but absent in TNBC cancer tissues.

EMT and migration of cancer cells is significantly favored (42, 44). A possible explanation resides in the loss of complex stability due to the downregulation of MALAT1 RNA molecule, in TNBC cells with respect to ER⁺ cells. Our results are in good agreement with the RNA-seq public dataset GSE58135, of breast cancer samples. In this dataset, we observed a significantly higher relative expression of CD133 in TNBC samples compared with ER⁺ samples, while, MALAT1 expression, although higher in comparison with normal tissues (not shown), exhibited a clear downregulating trend in TNBC tumors in comparison with the ER⁺ samples. In addition, the inverse correlation between MALAT1 and CD133 in ER⁺ samples was lost in TNBC samples, further supporting the functional repressive role of the MALAT1/HuR assembly on the D region of the CD133 gene. In conclusion,

Latorre et al.

**Figure 6.**

HuR-MALAT1 ribonucleic complex is present on CD133 gene D region in mammospheres derived from ER⁺ primary cells. A, RIP assay was performed on mammospheres derived from ER⁺ primary tumor cells (all patients) to evaluate MALAT1 RNA binding to HuR. The results are reported in the histogram as input percentage (% of input) of the fold enrichment. PCR was performed with or without retro transcription (RT) as amplification negative. Preimmunization serum (IgG) was used as precipitation negative control. The densitometry values were plotted as mean \pm SD from three different tumors. *, $P < 0.01$ in *t* test. B, RT-on-ChIP was performed on mammospheres derived from ER⁺ primary tumor cells (all patients) to evaluate MALAT1 RNA binding the chromatin bound to HuR. The results are plotted as input percentage (% of input) of the fold enrichment. PCR was performed with or without retrotranscription (RT) as amplification negative control. Preimmunization serum (IgG) was used as precipitation negative control. linc-CCND was used as negative control. The densitometric values were plotted as mean \pm SD from three different tumors. *, $P < 0.01$ in *t* test. C, ChIP assay was performed to amplify four CD133 gene regions, named A, B, C, and D bound to HuR or histone H3, on mammospheres derived from ER⁺ primary tumor cells (all patients). The results are reported in the histogram as input percentage (% of input) of the fold enrichment. PCR was performed with (RNase) or without RNase treatment (NT). Preimmunization serum (IgG) was used as precipitation negative control. Anti-histone H3 was used as positive control. Densitometric values were plotted as mean \pm SD from three different tumors. *, $P < 0.01$ in *t* test. D, ChIP was performed on mammospheres derived from ER⁺ primary tumor cells (all patients), TNBC primary tumor cells (all patients), MCF-7 and MDA-MB-231 cell lines to amplify CD133 gene D region bound to HuR (white bar) or histone H3 (gray bar). The results are reported in the histogram as input percentage (% of input) of the fold enrichment. Preimmunization serum (IgG) was used as precipitation negative control (black bar). Anti-histone H3 was used as positive control. Densitometric values were plotted as mean \pm SD from three different tumors. *, $P < 0.01$ in *t* test.

two novel observations can be gathered. The first one is the identification of a molecular mechanism underlying the CD133-dependent breast cancer EMT, in which the fine-tuning regulation of MALAT1 expression level modulates the insurgence of EMT traits with different outcome in TNBC cells and in ER⁺ cells. The second one is the description of a novel nuclear role for the RNA-binding protein HuR that, in association with the lncRNA molecule MALAT1, regulates the expression level of a key gene related to the EMT process. Clearly, to generalize this observation, high-throughput investigation combining HuR and MALAT1 association to the chromatin are warranted.

Disclosure of Potential Conflicts of Interest

No potential conflicts of interest were disclosed.

Authors' Contributions

Conception and design: E. Latorre, S. Carelli, G. Ghilardi, A. Inga, A. Gorio, A. Provenzani

Development of methodology: E. Latorre, V. D'Agostino, G. Ghilardi

Acquisition of data (provided animals, acquired and managed patients, provided facilities, etc.): E. Latorre, C. Zucal, G. Moro, A. Luciani, G. Ghilardi, E. Monti

Analysis and interpretation of data (e.g., statistical analysis, biostatistics, computational analysis): E. Latorre, S. Carelli, I. Raimondi, V. D'Agostino, E. Monti, A.M. Di Giulio, A. Gorio

Writing, review, and/or revision of the manuscript: E. Latorre, S. Carelli, I. Raimondi, V. D'Agostino, A. Luciani, G. Ghilardi, A. Inga, A. Gorio, A. Provenzani

Administrative, technical, or material support (i.e., reporting or organizing data, constructing databases): A. Gorio

Study supervision: G. Ghilardi, A.M. Di Giulio, A. Provenzani

Other (performed part of the presented experiments): I. Castiglioni

Acknowledgments

The authors thank Prof. Pier Paolo Di Fiore (IFOM-IEO Campus, Milan, Italy) for critically reading the manuscript, suggestions, and for providing reagents.

References

- Thiery JP, Acloque H, Huang RYJ, Nieto MA. Epithelial-mesenchymal transitions in development and disease. *Cell* 2009;139:871–90.
- Brabletz T. EMT and MET in metastasis: where are the cancer stem cells? *Cancer Cell* 2012;22:699–701.
- Puisieux A, Brabletz T, Caramel J. Oncogenic roles of EMT-inducing transcription factors. *Nat Cell Biol* 2014;16:488–94.
- Nomura A, Banerjee S, Chugh R, Dudeja V, Yamamoto M, Vickers SM, et al. CD133 initiates tumors, induces epithelial-mesenchymal transition and increases metastasis in pancreatic cancer. *Oncotarget* 2015;6:8313–22.
- Chen Y-S, Wu M-J, Huang C-Y, Lin S-C, Chuang T-H, Yu C-C, et al. CD133/ Src axis mediates tumor initiating property and epithelial-mesenchymal transition of head and neck cancer. *PLoS One* 2011;6:e28053.
- Ding Q, Miyazaki Y, Tsukasa K, Matsubara S, Yoshimitsu M, Takao S. CD133 facilitates epithelial-mesenchymal transition through interaction with the ERK pathway in pancreatic cancer metastasis. *Mol Cancer* 2014; 13:15.
- Grosse-Gehling P, Fargeas CA, Dittfeld C, Garbe Y, Alison MR, Corbeil D, et al. CD133 as a biomarker for putative cancer stem cells in solid tumours: limitations, problems and challenges. *J Pathol* 2013;229:355–78.
- Sheridan C, Kishimoto H, Fuchs RK, Mehrotra S, Bhat-Nakshatri P, Turner CH, et al. CD44+/CD24– breast cancer cells exhibit enhanced invasive properties: an early step necessary for metastasis. *Breast Cancer Res* 2006;8: R59.
- Han Z, Chen Z, Zheng R, Cheng Z, Gong X, Wang D. Clinicopathological significance of CD133 and CD44 expression in infiltrating ductal carcinoma and their relationship to angiogenesis. *World J Surg Oncol* 2015;13:56.
- Currie MJ, Beardsley BE, Harris GC, Gunningham SP, Dachs GU, Dijkstra B, et al. Immunohistochemical analysis of cancer stem cell markers in invasive breast carcinoma and associated ductal carcinoma in situ: relationships with markers of tumor hypoxia and microvasculature. *Hum Pathol* 2013;44:402–11.
- Liu TJ, Sun BC, Zhao XL, Zhao XM, Sun T, Gu Q, et al. CD133+ cells with cancer stem cell characteristics associates with vasculogenic mimicry in triple-negative breast cancer. *Oncogene* 2013;32:544–53.
- Ji P, Diederichs S, Wang W, Böing S, Metzger R, Schneider PM, et al. MALAT-1, a novel noncoding RNA, and thymosin beta4 predict metastasis and survival in early-stage non-small cell lung cancer. *Oncogene* 2003;22: 8031–41.
- Gutschner T, Diederichs S. The hallmarks of cancer: a long non-coding RNA point of view. *RNA Biol* 2012;9:703–19.
- Bernard D, Prasanth KV, Tripathi V, Colasse S, Nakamura T, Xuan Z, et al. A long nuclear-retained non-coding RNA regulates synaptogenesis by modulating gene expression. *EMBO J* 2010;29:3082–93.
- Yang L, Lin C, Liu W, Zhang J, Ohgi KA, Grinstein JD, et al. ncRNA- and Pc2 methylation-dependent gene relocation between nuclear structures mediates gene activation programs. *Cell* 2011;147:773–88.
- Lebedeva S, Jens M, Theil K, Schwanhäusser B, Selbach M, Landthaler M, et al. Transcriptome-wide analysis of regulatory interactions of the RNA-binding protein HuR. *Mol Cell* 2011;43:340–52.
- Zucal C, D'Agostino V, Loffredo R, Mantelli B, Thongon N, Lal P, et al. Targeting the multifaceted HuR protein, benefits and caveats. *Curr Drug Targets* 2015;16:499–515.
- Fan XC, Steitz JA. Overexpression of HuR, a nuclear-cytoplasmic shuttling protein, increases the *in vivo* stability of ARE-containing mRNAs. *EMBO J* 1998;17:3448–60.
- Hinman MN, Lou H. Diverse molecular functions of Hu proteins. *Cell Mol Life Sci* 2008;65:3168–81.
- Pece S, Tosoni D, Confalonieri S, Mazzarol G, Vecchi M, Ronzoni S, et al. Biological and molecular heterogeneity of breast cancers correlates with their cancer stem cell content. *Cell* 2010;140:62–73.
- Schaeren-Wiemers N, Gerfin-Moser A. A single protocol to detect transcripts of various types and expression levels in neural tissue and cultured cells: *in situ* hybridization using digoxigenin-labelled cRNA probes. *Histochemistry* 1993;100:431–40.
- Latorre E, Tebaldi T, Viero G, Sparta AM, Quattrone A, Provenzani A. Downregulation of HuR as a new mechanism of doxorubicin resistance in breast cancer cells. *Mol Cancer* 2012;11:13.
- Simon MD, Wang CI, Kharchenko PV, West JA, Chapman BA, Alekseyenko AA, et al. The genomic binding sites of a noncoding RNA. *Proc Natl Acad Sci U S A* 2011;108:20497–502.
- Cavallaro M, Mariani J, Lancini C, Latorre E, Caccia R, Gullo F, et al. Impaired generation of mature neurons by neural stem cells from hypomorphic Sox2 mutants. *Development* 2008;135:541–57.
- Huang RY-J, Wong MK, Tan TZ, Kuay KT, Ng AHC, Chung VY, et al. An EMT spectrum defines an anoikis-resistant and spheroidogenic intermediate mesenchymal state that is sensitive to e-cadherin restoration by a src-kinase inhibitor, saracatinib (AZD0530). *Cell Death Dis* 2013;4:e915.
- Latorre E, Castiglioni I, Gatto P, Carelli S, Quattrone A, Provenzani A. Loss of PKC δ /HuR interaction is necessary to doxorubicin resistance in breast cancer cell lines. *J Pharmacol Exp Ther* 2014;349:99–106.
- Mukherjee N, Lager PJ, Friedersdorf MB, Thompson MA, Keene JD. Coordinated posttranscriptional mRNA population dynamics during T-cell activation. *Mol Syst Biol* 2009;5:288.
- Kim HS, Wilce MCJ, Yoga YMK, Pendini NR, Gunzburg MJ, Cowieson NP, et al. Different modes of interaction by TIAR and HuR with target RNA and DNA. *Nucleic Acids Res* 2011;39:1117–30.
- Yoon J-H, Abdelmohsen K, Srikantan S, Yang X, Martindale JL, De S, et al. LincRNA-p21 suppresses target mRNA translation. *Mol Cell* 2012;47:648–55.
- Legnini I, Morlando M, Mangiacavalli A, Fatica A, Bozzoni I. A feedforward regulatory loop between HuR and the long noncoding RNA linc-MD1 controls early phases of myogenesis. *Mol Cell* 2014;21:1–9.
- Geisler S, Collier J. RNA in unexpected places: long non-coding RNA functions in diverse cellular contexts. *Nat Rev Mol Cell Biol* 2013;14: 699–712.
- West JA, Davis CP, Sunwoo H, Simon MD, Sadreyev RI, Wang PI, et al. The long noncoding RNAs NEAT1 and MALAT1 bind active chromatin sites. *Mol Cell* 2014;55:791–802.
- Eißmann M, Gutschner T, Hämmerle M, Günther S, Caudron-Herger M, Groß M, et al. Loss of the abundant nuclear non-coding RNA MALAT1 is compatible with life and development. *RNA Biol* 2012;9:1076–87.
- Gutschner T, Hämmerle M, Eissmann M, Hsu J, Kim Y, Hung G, et al. The noncoding RNA MALAT1 is a critical regulator of the metastasis phenotype of lung cancer cells. *Cancer Res* 2013;73:1180–9.
- Voss MJ, Möller MF, Powe DG, Niggemann B, Zänker KS, Entschladen F. Luminal and basal-like breast cancer cells show increased migration induced by hypoxia, mediated by an autocrine mechanism. *BMC Cancer* 2011;11:158.
- Tano K, Mizuno R, Okada T, Rakwal R, Shibato J, Masuo Y, et al. MALAT-1 enhances cell motility of lung adenocarcinoma cells by influencing the expression of motility-related genes. *FEBS Lett* 2010;584:4575–80.

Grant Support

This work was supported by CIBIO start-up grant, University of Trento, and by AIRC-MFAG [#17153] to A. Provenzani. E. Latorre was supported by the University of Trento fellowship and is now supported by the University of Milan fellowship.

The costs of publication of this article were defrayed in part by the payment of page charges. This article must therefore be hereby marked *advertisement* in accordance with 18 U.S.C. Section 1734 solely to indicate this fact.

Received July 28, 2015; revised February 8, 2016; accepted March 1, 2016; published OnlineFirst April 20, 2016.

Latorre et al.

37. Xu S, Sui S, Zhang J, Bai N, Shi Q, Zhang G, et al. Downregulation of long noncoding RNA MALAT1 induces epithelial-to-mesenchymal transition via the PI3K-AKT pathway in breast cancer. *Int J Clin Exp Pathol* 2015;8:4881–91.
38. Huarte M, Guttman M, Feldser D, Garber M, Koziol MJ, Kenzelmann-Broz D, et al. A large intergenic noncoding RNA induced by p53 mediates global gene repression in the p53 response. *Cell* 2010;142:409–19.
39. Bao X, Wu H, Zhu X, Guo X, Hutchins AP, Luo Z, et al. The p53-induced lincRNA-p21 derails somatic cell reprogramming by sustaining H3K9me3 and CpG methylation at pluripotency gene promoters. *Cell Res* 2015;25:80–92.
40. Wang X, Arai S, Song X, Reichart D, Du K, Pascual G, et al. Induced ncRNAs allosterically modify RNA-binding proteins in cis to inhibit transcription. *Nature* 2008;454:126–30.
41. Kagara N, Huynh KT, Kuo C, Okano H, Sim MS, Elashoff D, et al. Epigenetic regulation of cancer stem cell genes in triple-negative breast cancer. *Am J Pathol* 2012;181:257–67.
42. Kondaveeti Y, Guttilla Reed IK, White BA. Epithelial-mesenchymal transition induces similar metabolic alterations in two independent breast cancer cell lines. *Cancer Lett* 2015;364:44–58.
43. Nadal R, Ortega FG, Salido M, Lorente JA, Rodríguez-Rivera M, Delgado-Rodríguez M, et al. CD133 expression in circulating tumor cells from breast cancer patients: potential role in resistance to chemotherapy. *Int J Cancer* 2013;133:2398–407.
44. Guttilla IK, Phoenix KN, Hong X, Timauer JS, Claffey KP, White BA. Prolonged mammosphere culture of MCF-7 cells induces an EMT and repression of the estrogen receptor by microRNAs. *Breast Cancer Res Treat* 2012;132:75–85.

Cancer Research

The Journal of Cancer Research (1916–1930) | The American Journal of Cancer (1931–1940)

The Ribonucleic Complex HuR-MALAT1 Represses CD133 Expression and Suppresses Epithelial–Mesenchymal Transition in Breast Cancer

Elisa Latorre, Stephana Carelli, Ivan Raimondi, et al.

Cancer Res 2016;76:2626-2636. Published OnlineFirst April 20, 2016.

Updated version Access the most recent version of this article at:
doi:[10.1158/0008-5472.CAN-15-2018](https://doi.org/10.1158/0008-5472.CAN-15-2018)

Cited articles This article cites 44 articles, 7 of which you can access for free at:
<http://cancerres.aacrjournals.org/content/76/9/2626.full.html#ref-list-1>

E-mail alerts [Sign up to receive free email-alerts](#) related to this article or journal.

Reprints and Subscriptions To order reprints of this article or to subscribe to the journal, contact the AACR Publications Department at pubs@aacr.org.

Permissions To request permission to re-use all or part of this article, contact the AACR Publications Department at permissions@aacr.org.